Estimation of individual starch granule swelling under hydro-thermal treatment

François Deslandes, Artemio Plana-Fattori, Giana Almeida, Gabrielle Moulin, Christophe Doursat, Denis Flick

Estimation of individual starch granule swelling under hydro-thermal treatment

François Deslandes[a,b], Artemio Plana-Fattori[a,*], Giana Almeida[a], Gabrielle Moulin[a], Christophe Doursat[a], Denis Flick[a]

[a] *UMR Ingénierie Procédés Aliments, AgroParisTech, INRA, Université Paris Saclay, 91300 Massy, France*
[b] *MaIAGE, INRA, Université Paris-Saclay, 78350 Jouy-en-Josas, France*

Abstract

We propose an automatic algorithm to analyse the swelling kinetics of individual particles floating in a diluted suspension. Our approach is illustrated with a case study in which a diluted aqueous suspension of starch granules are submitted to various heating treatments. The evolution of modified waxy maize starch granules placed on a temperature-controlled stage was tracked using time-lapse light microscopy (one image per second). We relied on an automatic algorithm, developed for the present study, to estimate morphological and kinetic parameters for a large number of granules. Observations showed that above a given temperature, starch granules will evolve towards an equilibrium size. Due to variability of swelling kinetic, individual behaviour was different from the global one. These results suggest that modelling works should take into account the size heterogeneity and kinetic variability of starch granules.

Keywords: Modified waxy maize starch, swelling kinetics, size distribution, thermal history, hot-stage microscopy, image analysis

1. Introduction

Starch is vastly used as a thickener in various industrial processes mainly because it is abundant, easily available and cheap. Pharmaceutical, biomedical, polymer industry and food industry rely on starch for its ability to affect texture and viscosity (Noisuwan et al., 2007; Singh et al., 2007). In many applications involving food product such as dairy deserts, it is combined with milk and gelling agents which require pasteurization and sterilization to prevent microbial development. Those processes involve thermo-mechanical treatments during which starch granule swell by intake of water thereby affecting the rheological properties of liquid food products, heat transfer, and organoleptic characteristics (Dolan and Steffe, 1990; Tattiyakul and Rao, 2000; Doublier and Durand, 2008; Singh et al., 2007; Heertje, 2014; Anuntagool et al., 2017). Starch swelling is a key factor affecting food product transformation and the structural changes of starch under heat treatment has been the focus of many research efforts.

Starch exhibit a semi-crystalline structure composed of glucose polymers, mainly of linear amylose and branched amylopectin. Starch granules lose their semi-crystalline structure when heated in water. This transition from an ordered state to a disordered state is called gelatinization. This transition has been studied extensively (Marchant and Blanshard, 1978; Donovan, 1979; Evans and Haisman, 1982; Nakazawa et al., 1984; Biliaderis et al., 1986) but remains only partially understood (Ratnayake and Jackson, 2008). During hydrothermal treatments in excess water, intake of water leads to swelling up to several times the initial granule size and involves loss of birefringence (Singh et al., 2007). It can lead to the leaking of amylose and amylopectine in the liquid. Eventually, granules can also rupture and liberate all their content

*Corresponding author
Email address: artemio.planafattori@agroparistech.fr (Artemio Plana-Fattori)

Preprint submitted to Food Structure *June 5, 2019*

in the liquid. Those structural changes affect the volume fraction of starch granule in the suspension which impacts the rheological behaviour of the fluid. The viscosity of the fluid increases due to the increased volume fraction induced by swelling, and decreases after granule rupture. Research efforts have shown that the main factors affecting the suspension viscosity are a) the operating conditions, which drive granule swelling and the transformation of the product, b) the type of starch and c) its chemical properties. Chemically bonded starch is used to prevent granule rupture and the resulting loss of viscosity (Buléon et al., 1998; Choi and Kerr, 2004).

Models of starch swelling have been proposed over the years and include experimental models (Chen et al., 2007; Malumba et al., 2013), diffusion based models (Malumba et al., 2013; Desam et al., 2018) and first and second order kinetic models (Okechukwu and Anandha Rao, 1996; Lagarrigue et al., 2008). Model validation usually relies on laser diffraction granulometry with measurements usually obtained before and after thermal treatments. The main drawback of this approach is that it can only predict a global-scale information on starch swelling and does not allow the quantification of the variability that exists between individual granules.

A better understanding of the mechanisms driving and affecting starch swelling would enable the design of more reproducible processes and provide new insights on starch gelatinization. It will also improve the prediction of fluid flow and heat transfer in food processes involving starch which is a difficult task due to the importance of the temperature history on starch swelling (Lund and Lorenz, 1984).

Starch granule size distributions have been investigated by laser diffraction or hot-stage microscopy (Muñoz et al., 2015; Ovalle et al., 2013) but the kinetics of individual starch granules is generally omitted, due to the technical difficulty of tracking individual granules through various transitions. To provide new insights on starch granule swelling, we studied the kinetics and morphological changes affecting individual starch granules by developping a new particle detection procedure and relying on particle image tracking principles generally used in cell biology (Meijering et al., 2012).

The present study aims at a) quantifying individual starch granule heterogeneity, b) evaluating the influence of the heating rate on starch granule swelling kinetics and c) assessing the influence of individual granule kinetics on global kinetics.

We relied on time-lapse light microscopy observations of individual starch granules placed on a temperature controlled stage to describe both the kinetics of individual granules and the evolution of granule populations. Starch granule transformation during the heating stage lead to textural changes in images as well as movement. We developed an automated algorithm to track a significant number of individual granules through the complete heating period. We were able to estimate morphological and kinetic parameters of individual granules under several conditions of heat treatment. Statistical analysis of the data allowed us to quantify the effect of factors such as the heating rate and final temperature as well as to evaluate the impact of the initial granule size on swelling. This approach allowed us to quantify the heterogeneity of starch granule populations regarding kinetics and morphology.

2. Material and methods

2.1. Starch material and heat treatments

Chemically stabilized cross-linked waxy maize starch (acetylated adipate distarch, C*Tex 06205), provided by Cargill (Baupte, France), was used in 0.5 $g.kg^{-1}$ suspensions of starch in water. This starch is composed of 99% of amylopectin and less than 1% of amylose. This type of starch does not lead to disruption and no release of amylose content is expected. The samples were produced by adding starch powder to a 0.1 Mol of NaCl aqueous solution.

The present work focused on the observation of starch granules under white light, in order to study the evolution of the sizes and shapes of starch granules during thermal processing. Samples were placed on a Linkam LTS120 stage (Linkam Scientific Instruments, Surrey, UK). To ensure free swelling of starch granules, adhesive spacers were placed on the microscope slides (total thickness of 250 μm). Samples were observed under 50X magnification using an Olympus BX-51 microscope (Olympus Optical Co. Ltd., Tokyo, Japan). In order to assess the contours of each granule, observations were conducted under white light.

Images were acquired with a rate of one image per second using a Basler A102fc digital camera (Basler AG, Ahrensburg, Germany). Each observation is an 8 *bit* image of 1388×1038 $pixel^2$ which represents a 360.88×269.88 μm^2 area. The temperature was controlled with the Linksys32 software. In the first treatment (A), the temperature was increased from 50 °C to 90 °C with a rate of 5 °C per minute, in the second treatment (B) the temperature was increased from 50 °C to 90 °C with a rate of 10 °C per minute, and in the third treatment (C) the temperature was increased from 50 °C to 70 °C with a rate of 5 °C per minute. For the three treatments, observation started one minute before temperature increase and lasted 2 minutes after reaching the final temperature for treatments A and B, and 10 minutes in the case of treatment C. The final step of the heat treatment was chosen in order to assess the residual swelling under constant temperature.

2.2. Image processing

Starch granules appear as quasi-ellipses on 2-D light microscopy images. They initially exhibit uniform texture which changes during the heat treatment and becomes non-uniform after swelling as shown on Fig. 1. This textural change makes it difficult to track granules during swelling and to detect accurate contours. Starch granule can have a slight movement during the thermal treatment and may aggregate with surrounding granules, especially after swelling. To overcome these difficulties, we developed a two-step approach to separate touching granules and track them during the heat treatment. A morphological watershed algorithm allowed us to separate touching granules. Two binary images were used to identify granule contours. The first binary image was used to get accurate contours of the objects and the second one was used to obtain hole-free objects when thresholding and locate their general position.

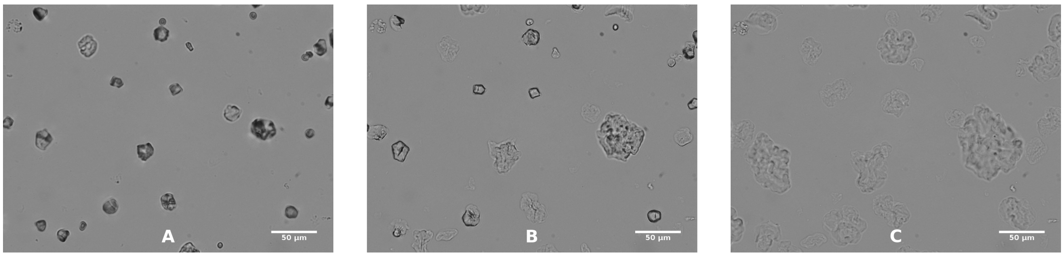

Figure 1: Raw images of starch granules after $0s, 180s$ and $540s$ at $5°C/min$, corresponding to 50°C (A), 75°C (B), 90 °C (C).

Individual starch granules were identified on the images through the following procedure, based on initial contours :

1. Subtract background with a rolling ball algorithm.
2. Create the first binary image by automatic thresholding (Ridler et al., 1978).
3. Create the second binary image by variance filtering (radius 5 pixels), contrast adjustment, automatic thresholding and hole filling.
4. The ultimate eroded points of the second binary image are labelled according to the initial contour if they lie inside of the contour.
5. A marker controlled morphological watershed procedure is applied on the distance image of the second binary image using the labelled ultimate eroded points as makers and the binary image as a mask.
6. The pixels labelled on the previous step are reported on the first binary image and the convex envelope of each label is used as the contour of the object.

The processing scheme is summed up in Fig. 2.

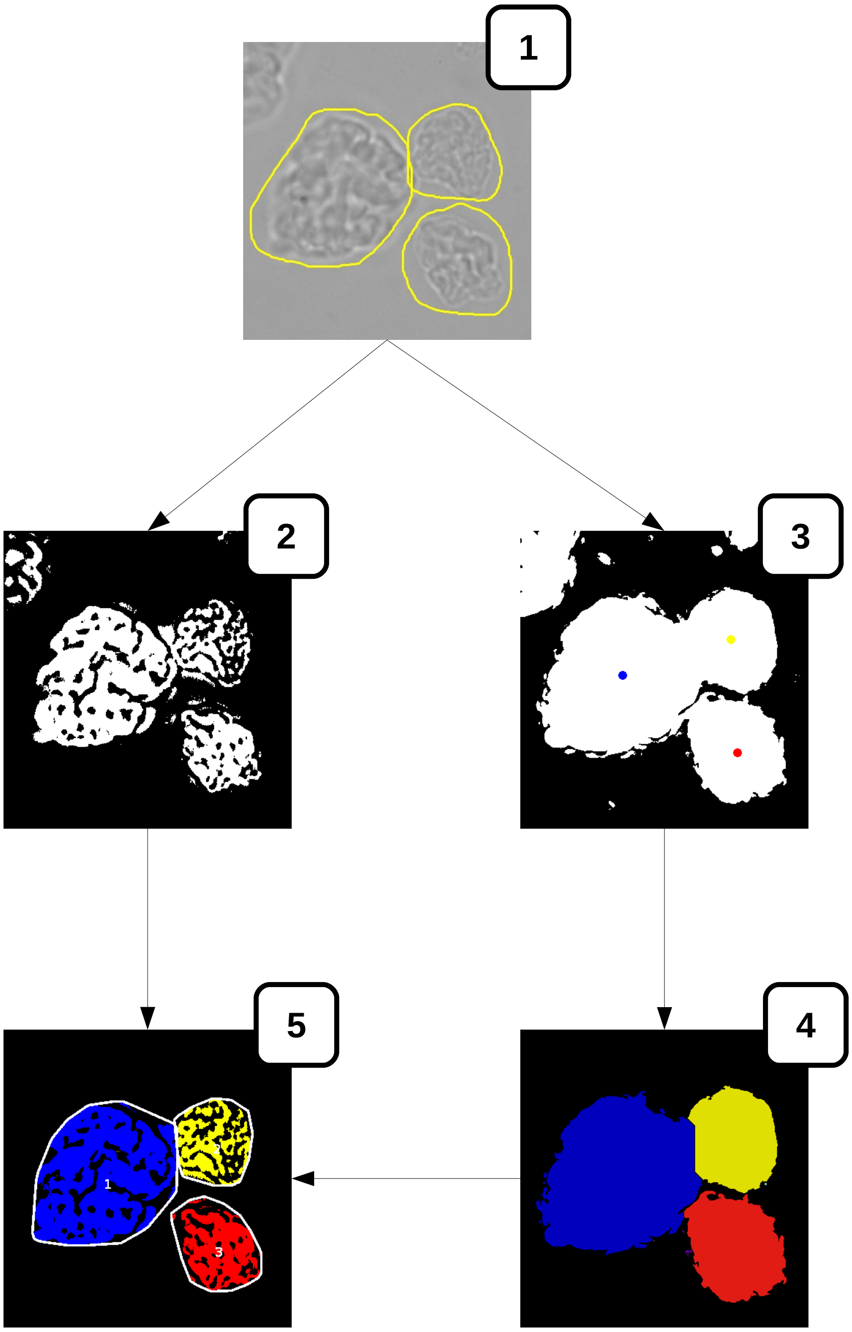

Figure 2: Image processing steps. 1- initial user-provided contour (yellow). 2- First binary image (possibly with holes) obtained by thresholding 3- Second binary image (without holes but with inaccurate contours) with the labelled ultimate eroded points 4- Label image obtained by flooding image 3. 5- Labels of 4 imposed on 2 and convex envelope (white).

Starch granules were tracked in image sequences using the contour identified in the previous image as an initial (inaccurate) contour. This linking procedure is a based on nearest neighbours principles and provides accurate results due to the small frame-to-frame displacement (Meijering et al., 2012). The first contour was user-provided. The integrity of the starch granules was automatically checked during the tracking step and faulty measurements were discarded in order to improve accuracy and not propagate errors. Using the contours provided by this procedure, the minimum and maximum Feret diameters were computed for each identified granule at each time step.

We note m and M the minimum and maximum Feret diameters of a granule (μm). We computed D, the size (μm) of the granule by taking the geometric mean of the Feret diameters :

$$D = \sqrt{Mm} \tag{1}$$

This procedure was implemented as a plugin for the ImageJ software (Schneider et al., 2012; Schindelin et al., 2012). The plugin relies on a morphological watershed algorithm (Legland et al., 2016).

2.3. Data analysis

2.3.1. Parameter estimation

The morphological and kinetics parameters, namely D_i and D_f the initial and final size (μm), λ the swelling rate (s^{-1}) and $t_{1/2}$ the half-swelling time (s), are estimated by least-squares fitting on the size evolution of individual granules of the following sigmoid curve :

$$\widetilde{D}(t) = \frac{D_f - D_i}{1 + e^{-\lambda(t - t_{1/2})}} + D_i \tag{2}$$

The beginning of the heating period is taken as the origin of time. Note that this empirical model is used in non-isothermal conditions, unlike the two-asymptotic logistic model presented in Malumba et al. (2013).

We define the aspect ratio as :

$$z = \frac{M}{m} \tag{3}$$

We estimate Δt the individual swelling duration by extrapolation of the tangent at the half-swelling time. It is related to the swelling rate λ by the following equation :

$$\Delta t = \frac{4}{\lambda} \tag{4}$$

We then define t_{onset}, the individual swelling onset time (s) by :

$$t_{onset} = t_{1/2} - \frac{\Delta t}{2} \tag{5}$$

We note T_{onset} the corresponding temperature (°C). We note $T_{\frac{1}{2}}$ the half-swelling temperature (°C).

2.3.2. Statistical analysis

Linear regression models were used to estimate the average growth D_f/D_i of starch granules after heat treatments as well as the average aspect ratio of the starch granule population. For model consistency, we dropped the intercept term.

Analysis of variance (ANOVA) models were used to evaluate the effect of the final temperature and heating rate on the variables describing individual starch granule evolution $D_f/D_i, T_{onset}$ and Δt.

The fit of all models were evaluated with F-tests and mean comparison were performed with Tukey tests. All tests were performed with a 5% risk. The quality of linear regression models was assessed with R^2 coefficients.

3. Results and discussion

To obtain kinetic and morphological information on individual granule swelling, we applied the procedure described in the previous section to 24 samples (18 for treatment A, 3 for treatment B and 3 for treatment C), which led to 206 starch granules tracks (142 for treatment A, 25 for treatment B and 38 for treatment C). Each track had between 300 and 660 time points. The image processing procedure presented in 2.2 was used to track the evolution of individual granules overtime and detect granule evolution. A user-provided initial rough contour was used to initialize the procedure. This procedure was fast and automated and required few user interactions for pre- and post-processing.

This procedure satisfactorily tracked granules through textural changes, aggregation and movement. The contours computed with this procedure were consistent with contours obtained manually in a previous contribution (Plana-Fattori et al., 2017) with an active contour snake algorithm (Andrey and Boudier, 2006), suggesting contours were accurate. The active contour snake algorithm does not allow the automatic tracking of particles over a collection of images. Each granule evolution was fitted with the sigmoid curve Eq. (2) and kinetic and morphological parameters were obtained. The sigmoid curve provided a good fit of the data. An example of this fit is given in Fig. 3. In this section, we used the fitted parameters to analyse the swelling behaviour of starch granule under heat-treatment.

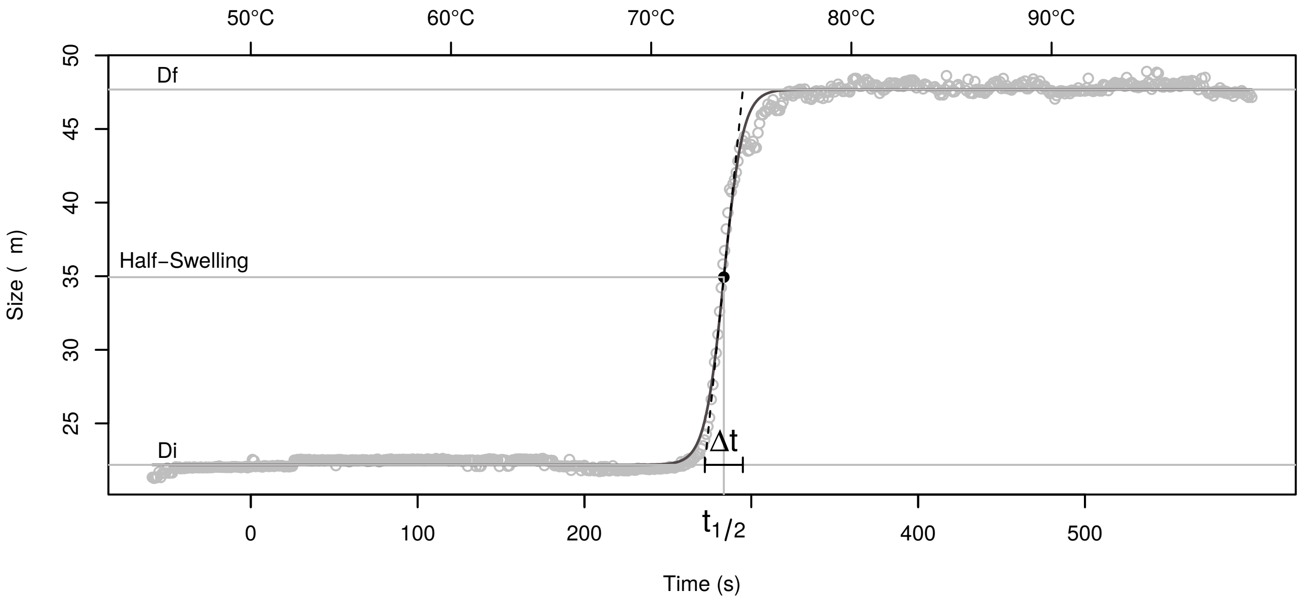

Figure 3: Fit of a sigmoid function on a granule evolution. The grey dots are the sizes of granules measured at each time point, during treatment A, and the black curve is the sigmoid fit. The temperature is constant at 50°C before $t = 0$ and constant after reaching the final temperature 90°C.

3.1. Swelling kinetics and morphology of individual granules

On 2-D light microscopy images, starch granules appeared as quasi-ellipsoidal and presented size heterogeneity as well as variability in swelling kinetics. This section is dedicated to analysis of the initial and final states and the analysis of kinetic parameters for treatment A.

We studied the initial size and aspect ratio to assess the heterogeneity of the starch granule population before the heat treatment and detect possible correlation between size and aspect ratio. Mean starch granule size was estimated to be 15.70 μm and we observed variability in sizes, as shown in Fig. 4A. This result is consistent with a previoulsy reported value of 16.3μm obtained by laser diffraction for similar modified waxy maize starch (Oliveira and Rao, 1997). This granule size is typically observed in starch that was submitted to pretreatment. The standard deviation of initial starch granule population was 4.60 μm, which reflects the initial size heterogeneity of starch granule. The number of granules smaller than the mean value was close to the number of granules larger than the mean value. The mean aspect ratio of the starch granules was initially 1.18 and was only weakly correlated with granule size (0.13). The initial aspect ratio distribution showed that the aspect ratio varies between granules, Fig. 4B. These results indicate that the starch granules are initially heterogeneous in size and in morphology. Smaller granules were not more spherical than larger granules and are as numerous as larger granules. Granules are only slightly elongated, which is consistent with previous imaging works on starch granules of several types (Singh et al., 2007), and with the commonly accepted assumption that starch granules are spherical.

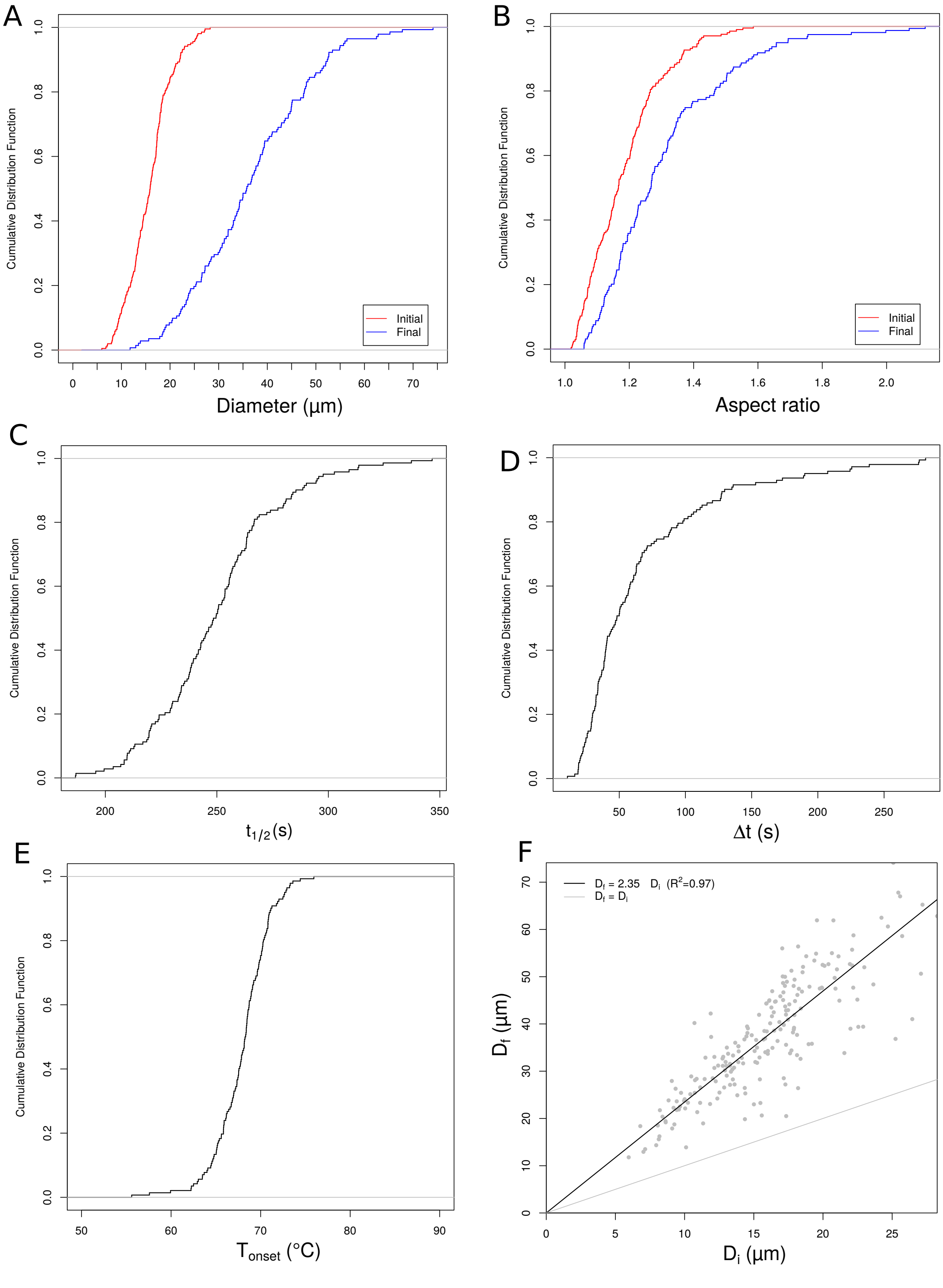

Figure 4: Cumulative distributions for treatment A of initial and final size (A), initial and final aspect ratio (B), half-swelling time (C), swelling duration (D) and swelling onset temperature (E). Final granule size after heat treatment versus initial size (F).

To study the effect of the heat treatment on size and aspect ratio, we compared the initial and final distributions of sizes and aspect ratios of treatment A. After swelling the aspect ratio slightly increased as shown on Fig. 4B. The initial and final aspect ratio were weakly correlated (0.08). The average aspect ratio increased from 1.18 initially to 1.30 after treatment.

Mean starch granule size increased from 15.70 to 36.50 μm after heat treatment. Similarly, standard deviation increased from 4.60 to 12.20 μm. Those results are also consistent with previously reported values on modified waxy maize starch (Oliveira and Rao, 1997). The final size distributions is shown on Fig. 4A and Fig. 4F shows the growth between the initial and final stages. Using a linear regression model between the final and the initial size, we estimated the average growth factor to be 2.33 ($R^2 = 0.97$). We observed a significant variability of the growth factor between granules. Heating increases size heterogeneity in the granule population, both in size and aspect ratio. The average aspect ratio is conserved after the heat treatment but individual granule aspect ratio may vary.

We investigated the kinetics of starch swelling using individual estimations of the swelling duration, half-swelling time and swelling onset temperature. We also studied the correlation of these parameters with the initial size of starch granule and found no significant link. The average swelling duration was 68 s and the standard deviation was 56 s. The large standard deviation can be explained by the skewed distribution of Δt. Most granules have swelling duration lower than 82 s, as shown on Fig. 4D. The average half-swelling time was 250 s (the corresponding temperature is 70.8 °C) and the standard deviation was 29 s for treatment A. The variability in half-swelling time, as shown in Fig. 4C, suggests that complete swelling of the starch granule population required more time than individual swelling. The half swelling time, size and swelling duration were weakly correlated. The swelling onset temperature distribution is shown on Fig. 4E. This parameter had a 68.0 °C mean and 3.0 °C standard deviation. We noticed that few granules had both a large swelling duration and large half swelling time. Under heat treatment, granules start swelling after a threshold temperature is reached and take some time to reach their equilibrium size. Both the swelling onset temperature and swelling duration are subject to variability between individual granules. These observations confirm that individual granules gelatinization temperature span over a 10-15°C range (Biliaderis, 2009). As a consequence of the variability in individual swelling onset temperature, the global kinetic of granule population is different from the individual granule kinetic. According to Reddy and Seib (2000) The swelling onset temperature of earlier granules is in the range of initiation of gelatinization for waxy maize starch measured by differential scanning calorimetry (DSC), and lower than the initiation of gelatinization for unmodified waxy maize starch. Average swelling tempererature is in the range of peak temperatures measured by DSC for waxy maize starch.

These results confirm that above a threshold temperature, starch granules swell until they reach an equilibrium size several times larger than their initial size. We showed that the growth factor is 2.35 on average but subject to variability induced by the heat treatment, that could not be explained by the data at our disposal. This variability could originate from differences in chemical composition between granules which may lead to differences in absorbed water (Patel and Seetharaman, 2010; Cai et al., 2014). Starch granule surface is known to be heterogeneous and presents small pores in the surface of waxy starch granule (approximately 1000 A in diameter) (*e.g.* (Fannon et al., 1992)). These pores were randomly distributed over the surface of the granule and often in clusters. These pores could improve the adsorption of water and partially explain different swelling kinetics between granules. This variability could be of interest when modelling the swelling of a starch granule population because it suggests that the swelling kinetic of the population is different from individual swelling.

3.2. Influence of operation conditions on the swelling duration

In this section, we study the influence of the final temperature and heating rate, on the parameters measured on individual granules. Results are summarized in Table 1.

	A 5°Cmin^{-1} $50 - 90$°C 142 granules	B 10°Cmin^{-1} $50 - 90$°C 25 granules	C 5°Cmin^{-1} $50 - 70$°C 38 granules	ANOVA Comparing factors A, B and C F-value	 p-value	Mean comparison
D_i	15.70 (4.60)	15.44 (4.47)	15.65 (5.04)	0.1448	0.8653	-
D_f/D_i	2.33 (0.40)	2.36 (0.39)	2.46 (0.41)	1.5517	0.2144	-
$t_{1/2}$	250 (29)	125 (12)	231 (35)	-	-	-
$T_{1/2}$	70.7 (2.4)	70.6 (1.9)	68.5 (1.4)	16.855	1.7e-7	$A \neq C$
Δt	68 (56)	30 (15)	65 (42)	6.0614	0.0028	$A \neq B$, $B \neq C$
t_{onset}	216 (37)	110 (14)	199 (36)	-	-	-
T_{onset}	68.0 (3.0)	68.3 (2.3)	66.6 (3.0)	5.1502	0.0066	$A \neq C$

Table 1: Mean parameters for treatments A, B and C and standard deviation in parenthesis. Analysis of variance was performed on $log\ \Delta t$. Multiple mean comparison at 5% with Tukey's HSD tests.

We observed, using analysis of variance, that the growth ratio D_f/D_i of starch granule was not affected by the heat treatment. The value of D_f/D_i can be considered statistically similar for all three treatments. The heating rate or the final temperature did not affect the equilibrium size. These results indicate that all three treatments lead to complete swelling, including treatment C which stopped heating after 70 °C and maintained this temperature constant during 10 minutes. It appears that D_f/D_i is not a robust parameter to assess the influence of the heating rate. These results suggest that there exist a temperature above which starch granule swelling is triggered and that, when heated above this temperature, granules will reach their equilibrium size, which is independent of the operating conditions.

The impact of the operating conditions on the swelling duration was also investigated with analysis of variance models. We observed that the final temperature had no impact on the swelling duration unlike the heating rate which had a significant impact on the swelling duration. We could verify that the swelling duration was twice as short for a 10 °C per minute heating rate than for a 5 °C per minute heating rate. This result shows that the heating rate is inversely proportional to the swelling duration, which indicates that the heating rate has a linear impact on the swelling rate in the temperature range considered in this study.

The relation between the operating conditions and swelling onset temperature was also investigated. We could not detect any proof that the swelling temperature was affected by the heat treatment. This result support the existence of a temperature threshold, independent of the heating rate but specific to each granule, above which granule start swelling.

3.3. Individual and global evolution of starch granule swelling

In this section, we compare the individual evolution of starch granules with the global evolution of the population.

Fig. 5A-B present the evolutions of the size distribution for treatment A. This information is aggregated for the population and is similar to that obtained by many authors (e.g. Lagarrigue et al. (2008)) by laser diffraction granulometry after a given heat treatment and a quick cooling. But here the possible artefact due to cooling and delay before measurement is avoided. The cumulative distributions (Fig 5.B) are shown is semi-log coordinates. The final distribution seems to be simply shifted, by a factor of about 2.33, in comparison with the initial one. Therefore one could imagine that all the granules swell by the same ratio with approximately the same kinetic.

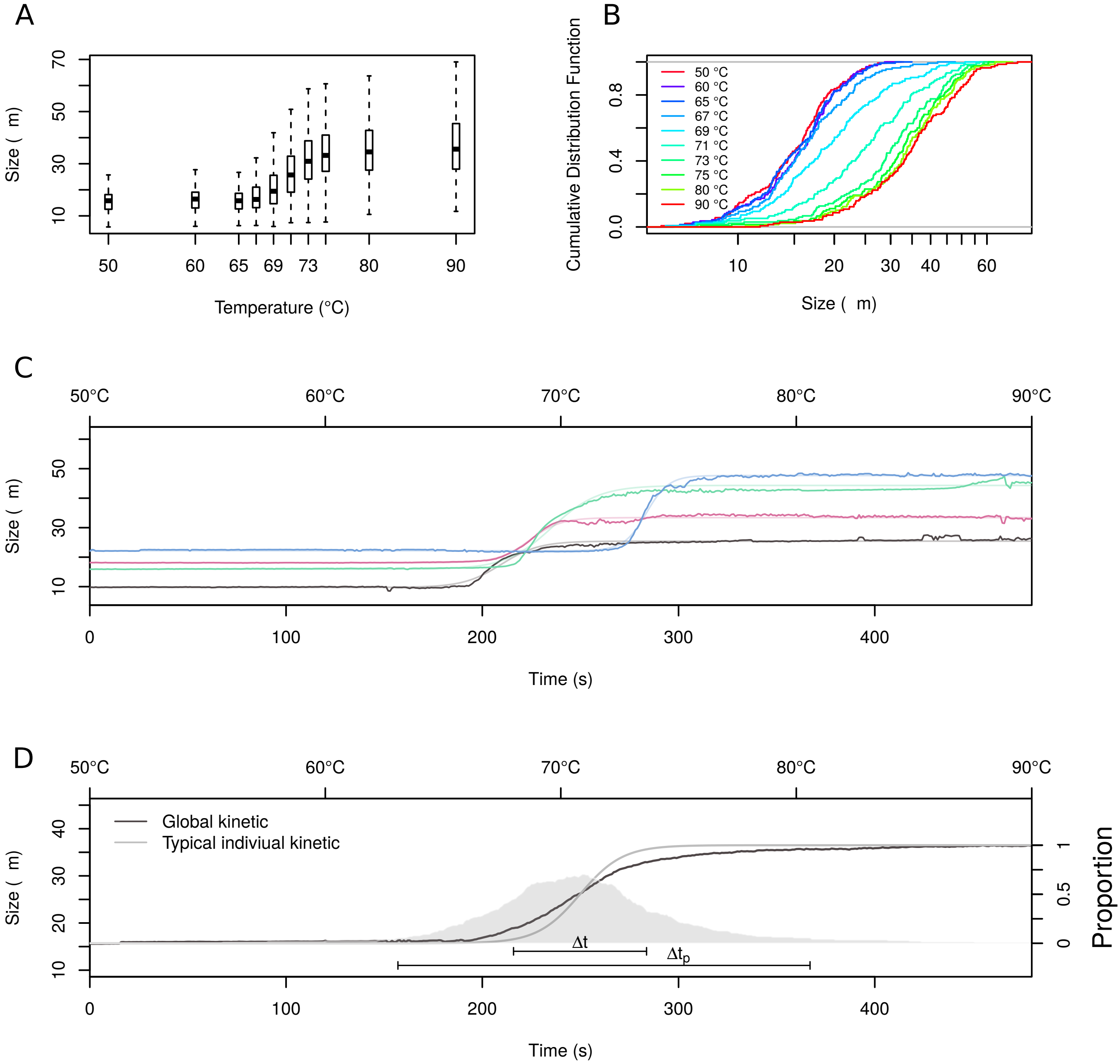

Figure 5: Distribution of starch granule size (A, B) during heat treatment A. Selected granule size evolutions during treatment A (C). Typical individual kinetic and global kinetic during heat treatment A (D). The grey area represents the proportion of granules in the process of swelling as a function of time.

In fact, from the individual granules evolutions, for which Fig. 5C gives some examples, we know that the granules do not swell with the same kinetic and do not grow with the same ratio. The onset temperature, T_{onset}, varies typically between 62 and 74°C and D_f/D_i varies typically between 1.5 and 3.1.

Fig. 5D presents the typical individual kinetic, defined as the sigmoid evolution of the diameter (Eq. 2) obtained with the mean values of the parameters obtained for the 142 granules of treatment A (Table 1). The duration of the swelling of the typical granule Δt is about $68s$.

Fig. 5D also shows the global kinetic, defined as the evolution of the average granule size of the population for treatment A. The average diameter increases over a period Δt_p of around $200s$. So it appears that the characteristic swelling time of the population is much larger that the characteristic swelling time of an individual granule; the latter cannot be obtained only from population information (e.g. laser diffraction granulometry). This result shows the relevance of tracking individual granule evolution.

The difference between these characteristic times is due to the variability of the swelling onset temperature and of individual swelling duration. Indeed, we observed that individual granules can start swelling at different temperatures and have different swelling rates. Fig 5D also presents the proportion of granules being in the swelling process. This proportion begins to be significant (more than 7% of granules between T_{onset} and $T_{onset} + \Delta t$) around 63°C ($157s$) and remains non negligible up to 80°C ($367s$). Therefore, the global kinetic extends over about $200s$.

Contrary to what could be assumed in the light of only population results, tracking individual granules shows that they do not all swell at the same time with the same ratio. They start to swell at different temperatures and with a variable ratio. Therefore, although they swell rapidly (on average in $68s$), the evolution of the average diameter of the population evolves more slowly (about $200s$).

4. Conclusion

We have implemented an image processing algorithm to track the evolution of individual particles. In the case of modified waxy maize starch granules under heat treatment, the tracking procedure overcomes the difficulty related to the change in texture during the swelling and is able to automatically process large number of images.

This approach allowed us to quantify the influence of two factors affecting starch granule swelling. Analysis of starch granule size before and after heat treatment revealed that size is about 2.35 times larger after heat treatment with a significant additional variability. Morphological analysis revealed that starch granules are slightly elongated with a mean aspect ratio of about 1.2 that is conserved after heat treatment. The aspect ratio was not correlated with granule size. Kinetics analysis revealed that the mean swelling duration is 68 s under a heating rate of 5 °C.min^{-1}. Variability was shown to exist in granule swelling time and swelling onset temperature; it might be related to to physico-chemical and structural variability between granules of a same population. The heating rate has a linear impact on the swelling rate which is inversely proportional to the swelling duration.

Swelling was complete at the end of the three heat treatments considered in this study, and we concluded that swelling continues until an equilibrium size is reached once a granule has been heated above a threshold temperature. The threshold temperature is specific to individual granules and is in the range of 62 to 74°C and 68°C on average. The equilibrium size was shown to be independent of the operating conditions.

Individual variability between starch granules was observed; as a consequence, individual granule swelling and population average swelling are different. Individual swelling can indeed be two or three times faster than the global swelling. These results were obtained for modified waxy starch which is known to have different stability and swelling kinetic unde hydrothermal treatment (Malumba et al., 2010, 2009; Stute, 1992; Tester and Morrison, 1990).

Starch is found as a population of particles of various initial size and structural features. The quantitative findings obtained in this study on individual granule kinetic represent a new step towards improved models of starch swelling and understanding individual variability between granules of a same population. Knowledge of the behaviour of individual granules can highlight competition for water and space between granules at high concentration. Linking initial and final diameters can also be helpful when studying rheology at high concentrations or when verifying hypothesis of swelling mechanisms.

Ongoing work includes the modelling of starch granule size as a function of time-temperature history, as a previous and necessary step for mechanistic representation of the evolution of the starch suspension under heat treatment. These results can be used to support hypothesis in the mechanistic modelling of starch swelling as well as the general understanding of starch interactions in food products (Considine et al., 2011; Matignon et al., 2014; Chung et al., 2012; Igoumenidis et al., 2018).

The generic features of this algorithm allows its application to track movement and changes in size and shape of other types of particles found in food science and technology.

Acknowledgments

Authors would like to thank Profs. Camille Michon and Gerard Cuvelier (AgroParisTech) for helpful discussions along our study.

Conflict of interests

The authors declare that there is no conflict of interests regarding the publication of this paper.

References

Andrey, P., Boudier, T., 2006. Adaptive active contours (snakes) for the segmentation of complex structures in biological images. Proceedings of the 1st Image-J User & Developer Conference, Luxembourg, 18-19 May 2006.

Anuntagool, J., Alvarez, G., Flick, D., 2017. Predictive model for viscosity development of modified rice starch suspension under unsteady temperature change. Journal of Food Engineering 209, 45–51.

Biliaderis, C. G., 2009. Structural transitions and related physical properties of starch. In: Starch (Third Edition). Elsevier, pp. 293–372.

Biliaderis, C. G., Page, C. M., Maurice, T. J., Juliano, B. O., 1986. Thermal characterization of rice starches: A polymeric approach to phase transitions of granular starch. Journal of Agricultural and Food Chemistry 34 (1), 6–14.

Buléon, A., Colonna, P., Planchot, V., Ball, S., 1998. Starch granules: structure and biosynthesis. International journal of biological macromolecules 23 (2), 85–112.

Cai, C., Zhao, L., Huang, J., Chen, Y., Wei, C., 2014. Morphology, structure and gelatinization properties of heterogeneous starch granules from high-amylose maize. Carbohydrate polymers 102, 606–614.

Chen, G., Campanella, O. H., Purkayastha, S., 2007. A dynamic model of crosslinked corn starch granules swelling during thermal processing. Journal of food engineering 81 (2), 500–507.

Choi, S.-G., Kerr, W. L., 2004. Swelling characteristics of native and chemically modified wheat starches as a function of heating temperature and time. Starch-Stärke 56 (5), 181–189.

Chung, C., Degner, B., McClements, D. J., 2012. Rheology and microstructure of bimodal particulate dispersions: Model for foods containing fat droplets and starch granules. Food Research International 48 (2), 641 – 649.

Considine, T., Noisuwan, A., Hemar, Y., Wilkinson, B., Bronlund, J., Kasapis, S., 2011. Rheological investigations of the interactions between starch and milk proteins in model dairy systems: A review. Food Hydrocolloids 25 (8), 2008–2017.

Desam, G. P., Li, J., Chen, G., Campanella, O., Narsimhan, G., 2018. A mechanistic model for swelling kinetics of waxy maize starch suspension. Journal of Food Engineering 222, 237–249.

Dolan, K. D., Steffe, J. F., 1990. Modeling rheological behavior of gelatinizing starch solutions using mixer viscometry data. Journal of Texture Studies 21 (3), 265–294.

Donovan, J. W., 1979. Phase transitions of the starch–water system. Biopolymers: Original Research on Biomolecules 18 (2), 263–275.

Doublier, J.-L., Durand, S., 2008. A rheological characterization of semi-solid dairy systems. Food Chemistry 108 (4), 1169–1175.

Evans, I., Haisman, D., 1982. The effect of solutes on the gelatinization temperature range of potato starch. Starch-Stärke 34 (7), 224–231.

Fannon, J. E., Hauber, R. J., BeMiler, J. N., 1992. Surface pores of starch granules. Cereal Chem 69 (3), 284–288.

Heertje, I., 2014. Structure and function of food products: A review. Food Structure 1 (1), 3 – 23.

Igoumenidis, P. E., Zoumpoulakis, P., Karathanos, V. T., 2018. Physicochemical interactions between rice starch and caffeic acid during boiling. Food Research International 109, 589–595.

Lagarrigue, S., Alvarez, G., Cuvelier, G., Flick, D., 2008. Swelling kinetics of waxy maize and maize starches at high temperatures and heating rates. Carbohydrate Polymers 73 (1), 148–155.

Legland, D., Arganda-Carreras, I., Andrey, P., 2016. Morpholibj: integrated library and plugins for mathematical morphology with imagej. Bioinformatics 32 (22), 3532–3534.

Lund, D., Lorenz, K. J., 1984. Influence of time, temperature, moisture, ingredients, and processing conditions on starch gelatinization. Critical Reviews in Food Science & Nutrition 20 (4), 249–273.

Malumba, P., Jacquet, N., Delimme, G., Lefebvre, F., Béra, F., 2013. The swelling behaviour of wheat starch granules during isothermal and non-isothermal treatments. Journal of Food Engineering 114 (2), 199–206.

Malumba, P., Janas, S., Masimango, T., Sindic, M., Deroanne, C., Béra, F., 2009. Influence of drying temperature on the wet-milling performance and the proteins solubility indexes of corn kernels. Journal of Food Engineering 95 (3), 393–399.

Malumba, P., Janas, S., Roiseux, O., Sinnaeve, G., Masimango, T., Sindic, M., Deroanne, C., Béra, F., 2010. Comparative study of the effect of drying temperatures and heat-moisture treatment on the physicochemical and functional properties of corn starch. Carbohydrate polymers 79 (3), 633–641.

Marchant, J., Blanshard, J., 1978. Studies of the dynamics of the gelatinization of starch granules employing a small angle light scattering system. Starch-Stärke 30 (8), 257–264.

Matignon, A., Moulin, G., Barey, P., Desprairies, M., Mauduit, S., Sieffermann, J.-M., Michon, C., 2014. Starch/carrageenan/milk proteins interactions studied using multiple staining and confocal laser scanning microscopy. Carbohydrate polymers 99, 345–355.

Meijering, E., Dzyubachyk, O., Smal, I., 2012. Methods for cell and particle tracking. In: Methods in enzymology. Vol. 504. Elsevier, pp. 183–200.

Muñoz, L. A., Pedreschi, F., Leiva, A., Aguilera, J. M., 2015. Loss of birefringence and swelling behavior in native starch granules: Microstructural and thermal properties. Journal of Food Engineering 152, 65–71.

Nakazawa, F., Noguchi, S., Takahashi, J., Takada, M., 1984. Thermal equilibrium state of starch-water mixture studied by differential scanning calorimetry. Agricultural and Biological Chemistry 48 (11), 2647–2653.

Noisuwan, A., Hemar, Y., Bronlund, J. E., Wilkinson, B., Williams, M. A., 2007. Viscosity, swelling and starch leaching during the early stages of pasting of normal and waxy rice starch suspensions containing different milk protein ingredients. Starch-Stärke 59 (8), 379–387.

Okechukwu, P. E., Anandha Rao, M., 1996. Kinetics of cowpea starch gelatinization based on granule swelling. Starch-Stärke 48 (2), 43–47.

Oliveira, J. C., Rao, M., 1997. Granule size distribution and rheological behavior of heated modified waxy and unmodified maize starch dispersions. Journal of texture studies 28 (2), 123–138.

Ovalle, N., Cortés, P., Bouchon, P., 2013. Understanding microstructural changes of starch during atmospheric and vacuum heating in water and oil through online in situ vacuum hot-stage microscopy. Innovative Food Science & Emerging Technologies 17, 135 – 143.

Patel, B. K., Seetharaman, K., 2010. Effect of heating rate at different moisture contents on starch retrogradation and starch–water interactions during gelatinization. Starch-Stärke 62 (10), 538–546.

Plana-Fattori, A., Almeida, G., Moulin, G., Doursat, C., Flick, D., 2017. An experimental study of the swelling behaviour of starch granules under heat treatment. International Journal of Food and Biosystem Engineering 5 (1), 23–30.

Ratnayake, W. S., Jackson, D. S., 2008. Starch gelatinization. Advances in food and nutrition research 55, 221–268.

Reddy, I., Seib, P., 2000. Modified waxy wheat starch compared to modified waxy corn starch. Journal of cereal science 31 (1), 25–39.

Ridler, T., Calvard, S., et al., 1978. Picture thresholding using an iterative selection method. IEEE trans syst Man Cybern 8 (8), 630–632.

Schindelin, J., Arganda-Carreras, I., Frise, E., Kaynig, V., Longair, M., Pietzsch, T., Preibisch, S., Rueden, C., Saalfeld, S., Schmid, B., et al., 2012. Fiji: an open-source platform for biological-image analysis. Nature methods 9 (7), 676.

Schneider, C. A., Rasband, W. S., Eliceiri, K. W., 2012. Nih image to imagej: 25 years of image analysis. Nature methods 9 (7), 671.

Singh, J., Kaur, L., McCarthy, O., 2007. Factors influencing the physico-chemical, morphological, thermal and rheological properties of some chemically modified starches for food applications—a review. Food hydrocolloids 21 (1), 1–22.

Stute, R., 1992. Hydrothermal modification of starches: The difference between annealing and heat/moisture-treatment. Starch-Stärke 44 (6), 205–214.

Tattiyakul, J., Rao, M., 2000. Rheological behavior of cross-linked waxy maize starch dispersions during and after heating. Carbohydrate Polymers 43 (3), 215–222.

Tester, R. F., Morrison, W. R., 1990. Swelling and gelatinization of cereal starches. i. effects of amylopectin, amylose, and lipids. Cereal chem 67 (6), 551–557.